Optica Applicata, Vol. X, No. 2, 1980

Waveguiding properties of thin film light guide made of $LiNbO_3$ single crystal *

WIESŁAW CIURAPIŃSKI, KRZYSZTOF GOŹDZIK, MIECZYSŁAW SZUSTAKOWSKI, BOGUSŁAW ŚWIETLICKI

Military Academy of Technology, Warsaw, Poland.

One of the most suitable materials for thin layer light modulation in the visible range is lithium niobate. A plate of lithium niobate of Y cut, thinned down to the thickness of order of 30 μm with one side deposited with a metal layer, creates an assymmetric waveguide. The light flux from a *He-Ne* laser introduced to the plate with the help of a prism of $BiGeO_{20}$ single crystal propagates in the direction of *x*-axis. The surface acoustic wave, propagating in the *z*-axis direction, is generated by two interdigital transducers positioned close to each other. This waveguide enabled a propagation of 70 modes but only four of them positioned in the central part of the spectrum transmit a significant light intensity. After switching-on the acoustic wave of frequency 60 MHz and 187 MHz a diffractions of Raman-Nath and Bragg types in all these four significant modes was observed.

Introduction

The fundamental element used to laser beam control in the optical integrated system are acousto-, electro- and magnetooptic modulators, deflectors and all kinds of optical switches [1-3]. These elements are usually produced in the form of planar light guides obtained by diffusion, ion implanation or thin film evaporation on the single crystal substrate [4]. The waveguiding properties of waveguides obtained in this way differ considerably from those of ideal light waveguides which are well represent by a thin single crystal layer. These differences result from technological difficulties connected with the production of an optically uniform light waveguide by means of the above methods.

In this paper the production possibility and waveguide properties of planar light waveguide made of lithium niobate plate are examined. The waveguiding effect was obtained with a distinct mode separation. Simultaneously, an effect of acoustooptic light modulation base on Raman-Nath or Bragg effects was observed.

Light-guiding properties of thin plate waveguide of $LiNbO_3$

The light-guide was made of a single crystal plate of lithium niobate 30 μm thick, deposited on a solid quartz substrate. Fig. 1 shows the waveguide design and the orientation of axes. The prism coupling the light beam from the *He-Ne* laser was made of rutile.

---

* This paper has been presented at the Fourth Polish-Czechoslovakian Optical Conference in Rynia (near Warsaw), Poland, September 19-22, 1978.

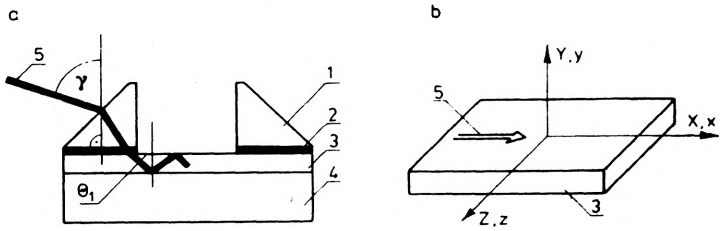

Fig. 1. a. Model of the system for which the calculations were carried out: 1 — prism, 2 — slit, 3 — light-waveguide, 4 — substrate, 5 — light beam. b. Orientation of crystallographic axis with respect to the coordinate system (γ — light acceptance angle, θ_1 — light propagation angle, X, Y, Z — crystal axes, x, y, z — axes of the accepted coordinate system)

In this way an asymmetric anisotropic light-guide was obtained. In such a light guide the characteristic equation for TE-modes has the form [5]:

$$Wk_0(n_1^1-n_f^2)^{1/2} = \arctan\left(\frac{n_f^2-n_s^2}{n^2-n_f}\right)^{1/2} + \arctan\left(\frac{n_f^2-n_c^2}{n_2-n_f^2}\right)^{1/2} + m\pi, \tag{1}$$

where: W — light-guide thickness,

$k_0 = 2\Pi/\lambda_0$ (λ_0 — light wavelength in vacuum),

n_f — effective refractive index of light-guide,

n_c — refractive index in the air,

n_1, n_2 — refractive indices of light guide along the x- and y-axes, respectively.

From the formula (1) the following parameters of the light propagation effect in the light-guide have been determined:

Θ_1 — light propagation angle,

γ — angle of light coupling via prism,

m — order of excited mode,

n_f — effective refractive index in the light-guide.

The results of calculations of these parameters for the thickness range 10-30 μm and $\lambda_0 = 0.6328$ are shown in fig. 2.

As it follows from fig. 2 the order of propagating modes within considered thickness range is very high and the mode number for a unit change n_f is very great.

It has been expected that due to some laser beam divergence as well as to fluctuations of refractive index n_f resulting, among others, from the surface treatment inaccuracies a great number of modes will be observed.

In fact, the mode structure obtained experimentally consisted of about 50-60 modes of very low intensity. A group of "strong" modes which may be distinguished in the central part of these "weak" modes will be called significant, hereafter. The number of these strong modes oscillates between 2 and 11, depending upon the cou-

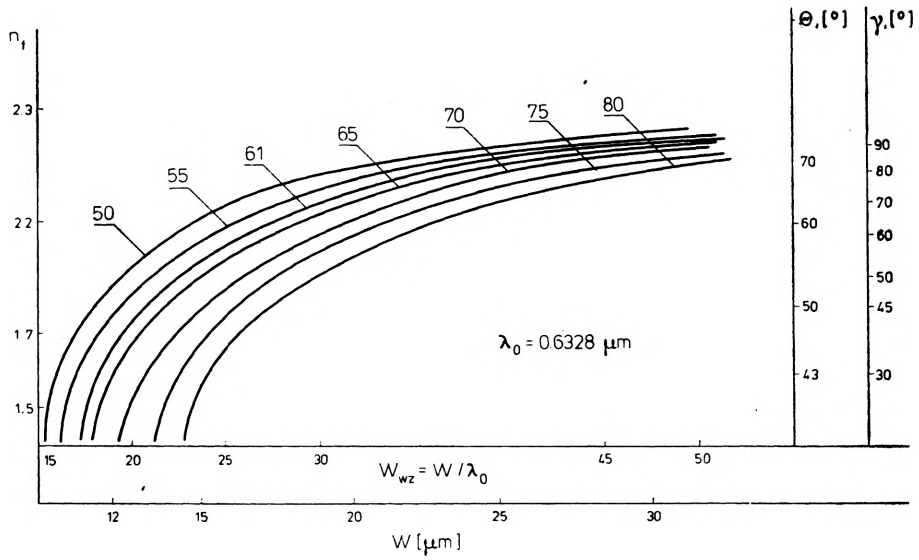

Fig. 2. Parameters of light propagation process in light waveguide of $LiNbO_3$ for several higher order modes. The numbers close to curves denote the mode numbers. n_f — effective refractive index, W — waveguide thickness, W_{wz} — relative thickness, γ — light acceptance angle, θ_1 — light propagation angle

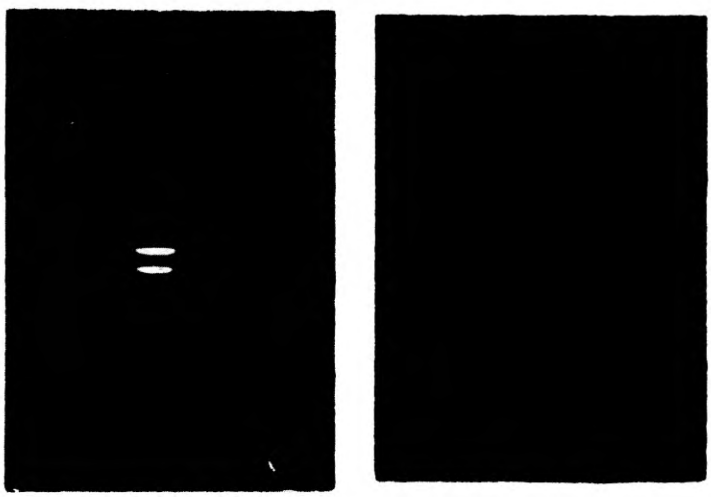

Fig. 3. Structure of significant modes: a) — two-mode case, b) four-mode case

pling angle γ. They contained above 95% of the intensity transmitted by the whole light waveguide. In fig. 3 two- and four-mode structures of significant modes are shown. The weak-mode background is not visible in the pictures.

The transmission efficiency η_t of the light waveguide examined (fig. 4) depends upon the coupling angle γ and the kind of excited modes. The coupling effectivity for TE-modes was 10 times higher than that for TM-modes.

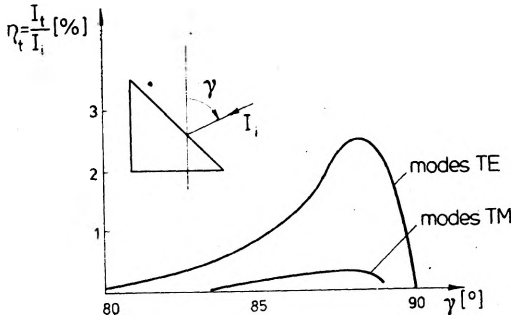

Fig. 4. Transmission efficiency of the Bragg diffraction vs. coupling angle: η_k — transmission efficiency, γ — acceptance angle, I_i — incidence beam intensity, I_i — emerging beam intensity

Acoustooptic interaction

The quantity characterizing the interaction effectivity is the diffraction efficiency defined as the ratio of the diffracted intensity to that of the incident beam. In the case of Bragg-type diffraction its efficiency depends upon the light propagation parameters and the acoustic wave in the following way [6]:

$$\eta = |\Gamma_{di}\cos\Theta_d|^2 L^2 \frac{\sin^2(TL)}{(TL)^2}, \tag{2}$$

$$\Gamma_{di} = \frac{v_n k}{v} \frac{\sin\Theta_i \sin\Theta_d \varepsilon_{11} I_{11} + \cos\Theta_i \cos\Theta_d \varepsilon_{33} I_{33}}{\int U_d U_d^* dx_2}, \tag{3}$$

where: v_n — propagation velocity of the n-th mode,
v — light velocity in the medium of which the modulator is made,
Θ_d — diffraction angle,
L — length of the interaction path,
U_d — diffraction angle,

$$I_{11} = \int p_{11g3} B_{q3} V_{q3} U_i U_i^* dx_2, \quad I_{33} = \int p_{33q3} B_{q3} V_{q3} U_i U_d^* dx_2$$

(p_{ijkl} — photoelastic constants, B_{q3} — amplitude of deformation, V_{q3} — distribution for deformation field).

In the system described the surface acoustic wave propagated along the z-axis. Assuming that this wave is of the Rayleigh-type with the displacement components u_2, u_3 [7], the terms I_{11}, I_{33} appearing in dependence (3) may be reduced to the form:

$$\begin{aligned} I_{11} &= \int B_3 p_{13} V_3 U_i U_i^* dx_2 \approx p_{13} B_3 K, \\ I_{33} &= \int B_3 p_{33} V_3 U_i U_d^* dx_2 \approx p_{33} B_3 K, \end{aligned} \tag{4}$$

where $K < 1$ is the coefficient representing the degree to which the electric and magnetic field distributions are overlapping. By virtue of the above expressions and the fact that $\sin \Theta_d \sim \lambda/\Lambda$ is of order of 10^{-3} the diffraction efficiency may be finally expressed:

$$\eta = \sin^2\left[\frac{v_n k}{v} LB_3 \cos^2(\Theta_i)\varepsilon_{33} p_{33} K\right]. \tag{5}$$

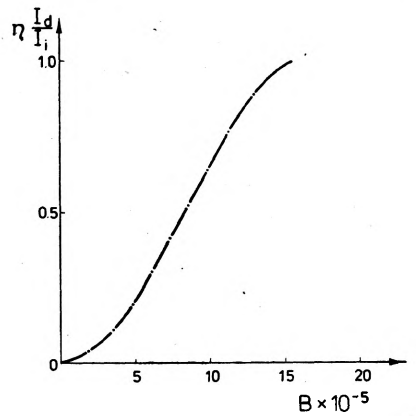

Fig. 5. Bragg diffraction efficiency vs amplitude of deformation: η — diffraction efficiency, I_i — incidence beam intensity, I_d — diffracted beam intensity

The theoretical dependence of the Bragg diffraction upon the deformation amplitude B_3 is shown in fig. 5. Similar considerations carried out for the diffraction of Raman-Nath-type allow to determine the efficiency in the form:

$$\eta = J_1^2\left[\frac{v_n k}{v} LB_3 p_{33} K\right]. \tag{6}$$

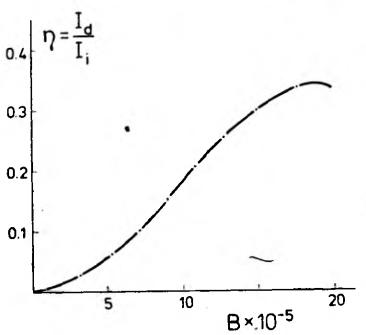

Fig. 6. Raman-Nath diffraction efficiency vs. amplitude of deformation (the significations are the same as in figure 5)

Fig. 6 presents the dependence of the diffraction efficiency of this type upon the deformation amplitude. In addition to the diffraction effect the acoustooptical

interaction evokes — in the case of anisotropic waveguide — a mode inversion in the part of scattered light. The change of indicatrix generated by the acoustic wave is

$$\Delta\varepsilon_{ij} = -\varepsilon_{ii}^2 p_{ijkl} S_{kl}. \tag{7}$$

In the system described the changes are expressed as follows:

$$\begin{cases} \Delta\varepsilon_{11} = -\varepsilon_{11}^2 (p_{12} S_2 + p_{13} S_3 + p_{14} S_4), \\ \Delta\varepsilon_{22} = -\varepsilon_{22}^2 (p_{11} S_2 + p_{13} S_3 + p_{12} S_4), \\ \Delta\varepsilon_{33} = -\varepsilon_{22}^2 (p_{44} S_4 - p_{41} S_2). \end{cases} \tag{8}$$

Hence, for the TE-modes (E_3, H_2, H_1) components of the induction vector have the form

$$\begin{bmatrix} D_1 + D_1 \\ D_2 + D_2 \\ D_3 + D_3 \end{bmatrix} = \begin{bmatrix} \varepsilon_{11} + \Delta\varepsilon_{11} & 0 & 0 \\ 0 & \varepsilon_{22} + \Delta\varepsilon_{22} & \Delta\varepsilon_{32} \\ \Delta\varepsilon_{32} & 0 & \varepsilon_{33} + \Delta\varepsilon_{33} \end{bmatrix} \begin{bmatrix} 0 \\ 0 \\ E_3 \end{bmatrix}. \tag{9}$$

The relation $D_3 = \Delta\varepsilon_{33} E_3$ determines the values of electric field scattered in the TE-mode structure, while the $D_2 = \Delta\varepsilon_{23} E_3$ component defines those in TE-mode structure. For low diffraction orders the two kinds of modes propagate under different angles and are easily distinguishable. In the case of multi-mode waveguide the angle differences between the TE- and TM-modes are very small and the mode inversion effect may be distinguished only by applying the polarization state analysis of scattered light.

Experimental examinations

The experimental examinations were carried out in the system shown in fig. 7. To the waveguide described in fig. 1 a pair of interdigital transducers exciting the acoustic surface wave has been added.

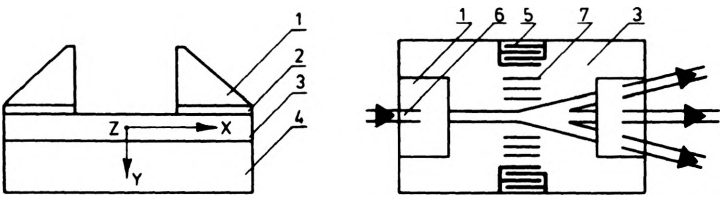

Fig. 7. Model of an acoustooptic thin film modulator: a) side wiev, b) top view. 1 — coupling prism, 2 — slit, 3 — light waveguide, 4 — substrate, 5 — transducer, 6 — light beam, 7 — acoustic wave (x, y, z — orientation of crystallographic axes)

In the experiment the following quantities were measured:

γ — angle of light coupling,
Θ_1 — diffraction angle,
η — diffraction efficiency.

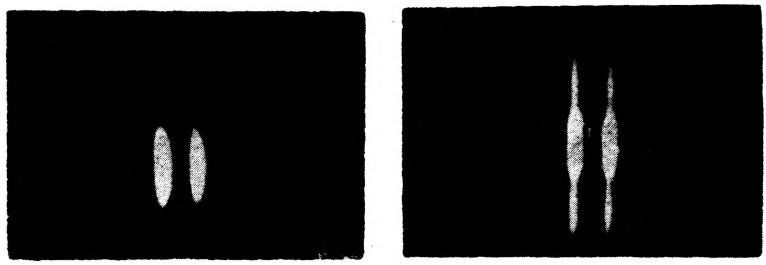

Fig. 8. Raman-Nath diffraction for two significant modes: a) before leading-in of the acoustic power, b) after leading-in of the power

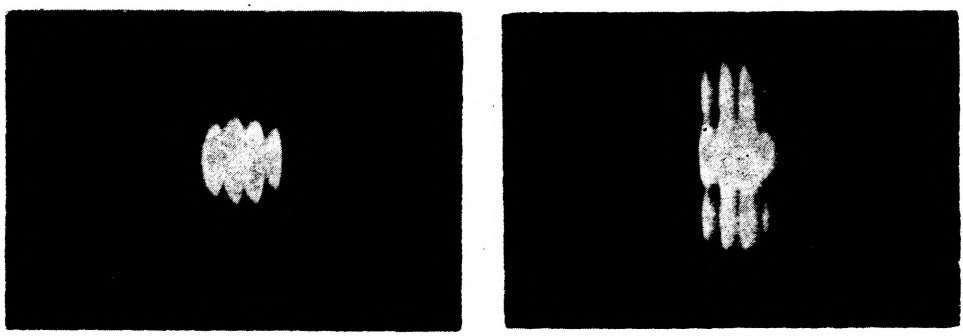

Fig. 9. Raman-Nath diffraction for four significant modes: a) before leading-in of the acoustic power, b) — after leading-in of the power

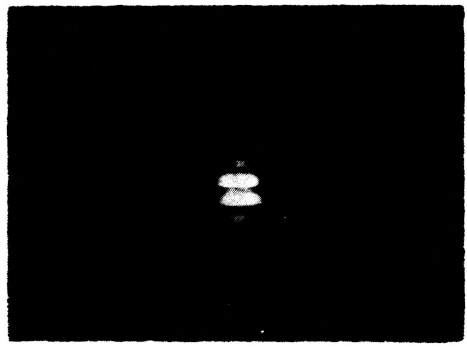

Fig. 10. Bragg diffraction for two significant modes

In the system described acoustooptic interaction effects were also observed. After exciting the acoustic surface wave an effect of Raman-Nath diffraction was obtained at the frequency 60 MHz and the effect of Bragg diffraction at the frequency 187 MHz. Figs. 8, 9 and 10 represent both the effects for different numbers of significant modes.

Experimental and theoretical dependences of the Raman-Nath diffraction angle upon the frequency are presented in fig. 11. Theoretical expectations concerning the changes in polarization of the light transmitted through the system have also found their experimental verifications.

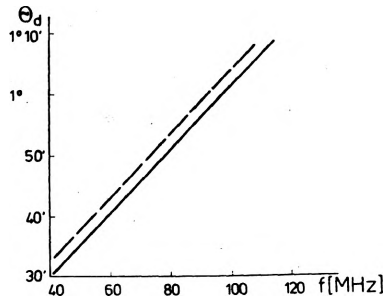

Fig. 11. Raman-Nath diffraction angles vs. the frequency, full line presents theoretical results, broken line shows the results of experiment (Θ_d — diffraction angle, f — acoustic wave frequency)

References

[1] KUHN L. et all., Appl. Phys. Lett. **17**, 265 (1970).
[2] SCHMIDT R. V. et all., Appl. Phys. Lett. **23**, 417 (1973).
[3] ZOLOTOV E. M., et all., Pisma v Zh. Tekh. Fiz. **3**, 226 (1977).
[4] TIEN P. K., Rev. Mod. Phys. **49**, 361 (1977).
[5] GONCHARENKO A. M., *Vvedenie v integralnuyu optiku*, Izd. Nauka i Tekhnika, Minsk 1975.
[6] *Vvedenie v integralnuyu optiku*, ed. M. Barnoski, Izd. Mir, Moskva 1977.
[7] FARNELL G. W., *Elastic Wave Propagation in Thin Layers*, ed. W. P. Mason, Academic Press, New York 1972.

Received, December 27, 1978,
in revised form May 7, 1979

Волноводовые свойства тонкослоистого светопровода из монокристалла $LiNbO_3$

Одним из наиболее соответствующих материалов для тонкослоистой модуляции света в видимой области является ниобат лития. Пластинка ниобата лития с сечением У, утоненная до толщины порядка 30 мкм с односторонно напыленным слоем металла образует несимметричный волновод. Поток света из лазера He-Ne, введённый в пластинку с помощью призмы из монокристалла $BiGe_{20}$, распространяется по направлению к оси x. Поверхностная звуковая волна, распространяющаяся по направлению к оси z генерируется двумя лежащими рядом межпальчатыми преобразователями. Описанный волновод дал возможность распространения около 70 модов, с тем, что только 4 мода, расположенных в средней части спектра переносили значащую интенсивность света. После включения звуковой волны частотой $f = 60$ и 187 МГц наблюдалась дифракция типа Рамана-Ната и Брагга во всех 4 значащих модах.